Study of Phase Separation of Poly(vinyl methyl ether) Aqueous Solutions with Rayleigh Scattering Technique

Wen Zhi Zhang,[†] Xu Dong Chen,*[,†] Wei-ang Luo,[†] Jin Yang,[†] Ming Qiu Zhang,*[,†] and Fang Ming Zhu[‡]

Key Laboratory for Polymer Composite and Functional Materials of the Ministry of Education, School of Chemistry and Chemical Engineering, Sun Yat-sen University, Guangzhou 510275, China, and Institute of Polymer Science, School of Chemistry and Chemical Engineering, Sun Yat-sen University, Guangzhou 510275, China

Received November 28, 2008; Revised Manuscript Received January 11, 2009

ABSTRACT: Phase separation and its kinetics of poly (vinyl methyl ether) (PVME) aqueous solutions was investigated by Rayleigh scattering (RS) technique in this work. Concentration dependence of the lower critical solution temperature and time dependence of phase separation were collected, respectively. The RS spectra revealed the transition of molecular conformation and aggregation of molecular chains in the course of phase separation. It was found that upon heating PVME chains changed from expanded coils to collapsed globules and then aggregated. In contrast, during cooling, the chain aggregates were initially swelled and followed by gradual dissociation, while the conformation of molecular chains finally returned to its original state. By means of Avrami equation and Arrhenius formula, apparent activation energy of phase separation of PVME aqueous solutions was estimated. Moreover, a model was proposed to describe the phase separation process.

Introduction

It is well-known that aqueous solutions of some water-soluble polymers are characterized by lower critical solution temperatures (LCST). The polymers are soluble at low temperatures, but heating above their LCSTs would result in phase separation. Thermosensitive water-soluble polymers, such as poly(N-substituted acrylamide)s[1−3] and poly(vinyl ether)s,[4−7] have been extensively investigated in the past two decades due to their unique properties and potential biotechnological applications. Poly(vinyl methyl ether) (PVME) has a lower critical solution temperature at moderate temperature range around 35 °C,[8−10] which makes it suitable for drug delivery.[11,12]

On molecular level, phase separation in PVME solutions was assumed to be a macroscopic manifestation of a coil-globule transition followed by aggregation.[13] The transition in PVME/water systems might probably be associated with competition between hydrogen-bonding and hydrophobic interactions.[14] PVME has hydrophilic ether groups (which can stabilize the aqueous solution by forming hydrogen bonds with the neighboring water molecules[15]) and hydrophobic methyl groups (which can destabilize the solution by altering normal water structure near the chains[16]). The hydrophobic interaction monotonously increases during heating, which finally breaks the balance between the hydrogen bonding and hydrophobic interaction and induces phase separation.[8,17] The onset of phase separation for PVME solutions is located in the temperature range of 32−35 °C, as determined by modulated-temperature differential scanning calorimetry.[18]

In recent years, phase transition of PVME aqueous solutions has been widely studied by differential scanning calorimetry,[19−22] Fourier transform infrared (FT-IR) spectroscopy,[8,17] Raman spectroscopy, [23]^{1}H NMR,[13,24] and small-angle neutron scattering.[25−27] In general, differential scanning calorimeter is able to measure the amount of heat absorbed in the whole sample during phase transition but cannot provide information about molecular aggregation in PVME solution. To reveal the inherent nature of phase separation of PVME solution in molecular terms, the information about hydration of individual chemical groups is necessary. The status changes of individual chemical groups on the polymer chain can be monitored by infrared and Raman spectroscopy. Besides, ^{1}H NMR has also been used to study the molecular dynamics mechanism of phase separation of the PVME solution. Nevertheless, ^{1}H NMR and small-angle neutron scattering need expensive equipment and complicated testing processes.

As an analytical method, the response Rayleigh scattering (RRS) technique has been the focus of interest of many studies for its high sensitivity, convenience in performance, simplicity, and rapidity. It proved to be a promising technique not only for determination of biological macromolecules,[28−30] trace amounts of inorganic ions,[31] and nanoparticles,[32] but also for study of aggregation and assembly of biological and chemical species.[33,34] In addition, it can be used to reveal interactions between biopolymers and their probes.[35] When the scattering peaks are away from the absorbance envelopes of scattering system, the enhanced scattering acquired with the same procedure as that of RRS is ascribed to Rayleigh scattering (RS).[36] Rayleigh scattering is able to characterize aggregation in polymer solution by a single parameter: RS intensity (I_{RS}), which can be considered as an index of the degree of PVME aggregation. In this context, the intensity of Rayleigh scattering is related to the changes in macromolecular phase behavior.

In order to gain deeper insight into the inherent mechanism and kinetics of phase separation of PVME aqueous solution at molecular level, the present work applies RS spectra to investigate transition of molecular conformation and aggregation of macromolecular chains during phase separation of PVME solution. Molecular chain diffusion and aggregation of PVME solution are traced by studying temperature, concentration and time dependent RS spectra of the polymer during one heating and cooling cycle. The RS spectra are collected by simultaneously scanning the excitation and emission monochromators of a conventional spectrofluorimeter with $\Delta\lambda = 0$ nm.[37,38]

* Corresponding authors. E-mail: cescxd@mail.sysu.edu.cn (X.D.C.); ceszmq@mail.sysu.edu.cn (M.Q.Z.).

[†] Key Laboratory for Polymer Composite and Functional Materials of the Ministry of Education, School of Chemistry and Chemical Engineering, Sun Yat-sen University.

[‡] Institute of Polymer Science, School of Chemistry and Chemical Engineering, Sun Yat-sen University.

10.1021/ma802671a CCC: $40.75
Published on Web 02/17/2009

Theoretical Background. Rayleigh scattering is an elastic scattering of light or other electromagnetic radiation by particles. When the incident light passes through a solution containing aggregates, the intensity of light scattering enhances because of the scattering of particles. According to law of Rayleigh scattering, the intensity of scattering light has been proposed as[39]

$$I = \frac{24\pi^3 v^2}{\lambda^4}\left(\frac{{n_1}^2 - {n_0}^2}{{n_1}^2 + 2{n_0}^2}\right)^2 \left(\frac{N}{V}\right) I_0 \quad (1)$$

where I is the intensity of scattering light, I_0 is the intensity of the incident light, λ is the wavelength of the incident and scattered light, N/V is the number of the scattering particles per unit volume, v is the volume of one particle, n_1 and n_0 are the refractive indices of the particle and surrounding medium, respectively. When RS spectrum of the sample is recorded with synchronous scanning at $\lambda_{ex} = \lambda_{em}$ (i.e., $\Delta\lambda = 0$ nm), the RS intensity can be calculated with the following expression:[36]

$$I_{RS}(\lambda_0) = \frac{24\pi^3 v^2}{{\lambda_0}^4}\left(\frac{{n_1}^2 - {n_0}^2}{{n_1}^2 + 2{n_0}^2}\right)^2 \left(\frac{N}{V}\right) I_0(\lambda_0) = K\rho v^2\left(\frac{N}{V}\right) = K\rho v^2\left(\frac{m'}{\rho v V}\right) = Kv\left(\frac{n'M}{V}\right) = KvMc \quad (2)$$

Here λ_0 is the wavelength of the incident and scattered light, $I_{RS}(\lambda_0)$ is the intensity of Rayleigh scattering at λ_0, $I_0(\lambda_0)$ is the intensity of the incident light at λ_0, m' is the mass of the scattering substance, ρ is the density of the scattering substance, and n', M, and c are amount of substance, molar mass, and molar concentration of the scattering material, respectively. $K = 24\pi^3 I_0(\lambda_0)/\rho{\lambda_0}^4[({n_1}^2 - {n_0}^2)/({n_1}^2+2{n_0}^2)]^2$, supposing that the determination conditions and the medium are fixed.

It can be seen that $I_{RS}(\lambda_0)$ is proportional to N/V and v under certain conditions. That is, the intensity of scattering light depends on the number of the scattering particles or aggregates per unit volume and the volume of one aggregate. When the intensity of RS increases in phase separation process, v reflects the extension of particle size. On the other hand, v can show the decrease of particle size when the intensity of RS decreases. Thus, RS can be applied to characterize the aggregation and extension of macromolecular chains during phase separation by monitoring the change in geometric size of particle from the RS intensity variances.

Experimental Section

Materials and Samples Preparation. PVME was purchased from Sigma-Aldrich as a 50 wt % aqueous solution. Its average molecular weight was roughly estimated by gel permeation chromatography to be 90 000. The polymer was used without any purification. The solution was further diluted to solutions of different concentrations (0.75, 1.2, 1.5, 3.0, 4.5 w/v %) with doubly distilled and deionized water. Prior to the experiments, PVME solutions were incubated for seven days below the LCST for equilibration.

Apparatus. RS measurement was performed on a Cary Eclipse Fluorescence Spectrophotometer (Varian, Inc., America) equipped with a Xenon flash lamp, a R928 photomultiplier detector and dual monochromators. In addition, the spectrophotometer possesses a single cell Peltier holder, which is an electronically controlled thermostating single cell accessory capable of controlling the temperature within ± 0.1 °C. The variable temperature measurement in the range of 0−100 °C was carried out by using this unit. RS spectra of the systems were recorded from 260 to 700 nm with synchronous scanning at $\lambda_{ex} = \lambda_{em}$ (i.e., $\Delta\lambda = 0$ nm).

UV−vis absorption spectra of PVME solutions were collected by a UV-3150 spectrophotometer (Shimadzu Corporation, Japan). The slit width was 1 nm during the measurements.

Procedure. The sample was put into the single cell Peltier holder where the temperature was set at 25 °C. After twenty minutes,

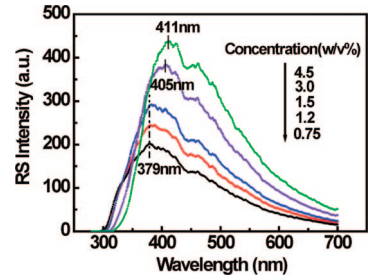

Figure 1. RS spectra of PVME aqueous solutions with different concentrations (C = 0.75−4.5 w/v %) at 25 °C.

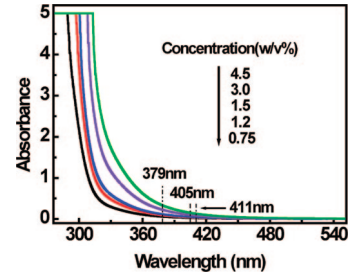

Figure 2. Absorption spectra of PVME aqueous solutions with different concentrations (C = 0.75−4.5 w/v %).

Rayleigh scattering spectra were measured by synchronous scanning at $\Delta\lambda = 0$ nm. Then, the sample was heated from room temperature to 36 °C at a heating rate of 0.5 °C /min, in which there was a time interval of 10 s for each increase of 0.5 °C. The slit (ex/em) width was 5 nm/5 nm for the measurements of RS spectra of PVME aqueous solutions with different concentrations at 25 °C, and RS spectra of PVME solution (C = 1.5 w/v %) during temperature rising. The slit (ex/em) width of other measurements was 1.5 nm/2.5 nm.

Results and Discussion

RS and Absorption Spectra of PVME in Aqueous Solutions. Aggregation state of molecular chains in polymer solutions changes with their concentration. According to the characteristics of segment density,[40] polymer solutions can be classified into three categories: dilute, semidilute, and concentrated. For the transitions from dilute to semidilute to concentrated regimes, there exist two critical concentrations, denoted as C* and C$^+$, respectively. At very low concentrations, the polymer chains exist as isolated coils that are far apart, and intermolecular interaction is very weak. With a rise in concentration, in semidilute solution, linear chains begin to overlap and interpenetrate each other; while in concentrated solution, polymer chains impenetrate and form entanglement network where chain segments are uniformly distributed, and there is certain interaction between the two adjacent molecules.

Figure 1 shows RS spectra of PVME aqueous solution with different concentrations recorded at 25 °C. The spectral characteristics of all the solution systems are similar. The maximum scattering wavelengths, λ_{max}, of solutions (C = 0.75, 1.2, 1.5 w/v %) is located at 379 nm, and λ_{max} of solutions (C = 3.0, 4.5 w/v %) appear at 405 and 411 nm, respectively. It can be seen that I_{RS} is greatly enhanced with an increase in PVME concentration, and λ_{max} of solutions exhibits a red-shift (from 379 to 405 nm, and to 411 nm). The increase of I_{RS} should be due to the rise in molecular number of PVME per unit volume, along with increasing concentration. In addition, the increase in absorbance of the studied system results in red-shift of λ_{max} of the solutions.

Figure 2 displays the absorption spectra of PVME aqueous solutions with different concentrations (C = 0.75−4.5 w/v %).

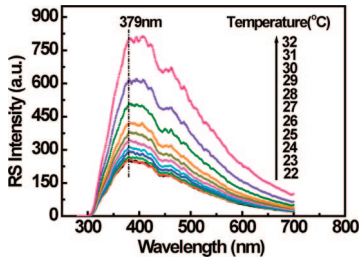

Figure 3. RS spectra of PVME solution (C = 1.5 w/v %) recorded during heating.

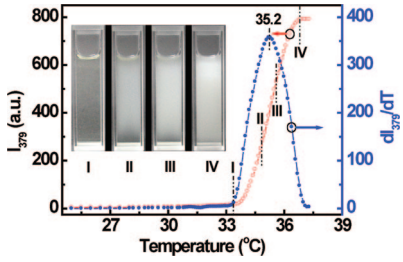

Figure 4. Temperature dependence of RS spectrum intensity at 379nm (I_{379}) of PVME solution (C = 1.5 w/v %), and the differential curve of I_{379} against temperature. The inset gives visual inspection of the phase separation during heating.

It can be seen that PVME exhibits absorption band below 360 nm, whereas the absorbance approaches zero in the range over 400 nm. Moreover, the absorbance gradually increases and the absorption band is strengthened with increasing concentration. The band strengthening is due to the increase of absorbance. By comparing Figure 1 and Figure 2, we find that the maximum Rayleigh scattering intensities of PVME solutions with different concentrations appear at 379−411 nm, which are all located at the red side of the absorption band of the solutions. It implies that the maximum scattering peaks becomes perceivable where the absorption decreases, ascribed to Rayleigh scattering.[36]

Temperature Dependence of RS Spectra of PVME Solutions. Temperature dependence of RS spectra of PVME solution (C = 1.5 w/v %) is presented in Figure 3. It can be observed that I_{RS} increases with increasing temperature, and at room temperature, λ_{max} appears at 379 nm. When temperature is raised to 32 °C, λ_{max} begins to show a slight red-shift. The increase in I_{RS} results from the fact that the main chains of PVME (methyl groups) dehydrate during heating. When water molecules clustering around the C−H groups break away, hydrogen bonding network formed between C−H groups of PVME chain and water molecules is disrupted, and conformation of C−H main chains would change accordingly,[41] inducing a slight red-shift of the maximum scattering wavelength at higher temperature. Considering the sensitivity of detection, the maximum scattering wavelength is selected for the further work.[42]

Figure 4 shows temperature dependence of RS spectrum intensity at 379nm (I_{379}) of PVME solution (C = 1.5 w/v %) during heating. Clearly, I_{379} is almost constant at the initial stage of heating, and then presents a sharp increase within higher temperature regime, corresponding to a drastic change in polymer concentration in the polymer-rich phase.[18] Finally, I_{379} reaches a plateau, suggesting that phase separation comes into the last stage. In such a manner, the RS spectrum intensity at the maximum scattering wavelength exhibits its feasibility in serving as an indication of phase separation extent of PVME solution. The higher extent of phase separation, the stronger the RS.

During the phase separation, main chains of PVME begin to dehydrate, and their conformation undergoes a "coil−globule" transition, inducing dehydration of the hydrophilic side groups.[41] These changes of main chain make the I_{379} begin to gradually increase, which can be considered as the signal of the onset of phase separation. Subsequently, ether oxygens that have strong hydrogen bond with water below LCST are wrapped by the hydrophobic CH group of the main chains and dehydrate,[17] and molecular chains start to aggregate, leading to the sharp increase of globule size. According to the coalescence-induced coalescence mechanism of phase separation,[43−45] any process of domains coalescence that induces hydrodynamic flow would push other domains toward each other and result in further coalescence events. Such a "chain-reaction process" is not self-sustained and finally stops.[46] Therefore, we conclude that diffusion and aggregation of molecular chains account for the drastic increase in I_{379}.

Figure 4 also gives temperature derivative of I_{379} of PVME solution, which factually represents the rate of phase separation. The data demonstrate that the phase separation is first accelerated and then decelerated with temperature, offering the peak rate at 35.2 °C. The inset photos taken at different temperatures (i.e., I, II, III, and IV) further visualize the phase separation process. Obviously, the solution is transparent before phase separation. From I to II, PVME molecular chains begin to collapse and partially aggregate, so that the solution becomes cloudy when temperature is raised to 34.9 °C. When temperature is further increased, the solution is more turbid because of continuous diffusion and aggregation of PVME chains, and rapid increase in globule size.

To gain an in-depth understanding of the collapse and aggregation of PVME chains in the process of phase separation, concentration dependence of phase separation of PVME solutions was studied. Figure 5 displays the temperature dependence of normalized RS intensities (at the maximum scattering wavelength) of PVME solutions with different concentrations. Accordingly, the onset temperatures of phase separation (T_p) are determined, which well agree with those reported in the literature.[22,47,48] From Figure 5 it is seen that T_p decreases with a rise in solution concentration. This can be attributed to the overlap and entanglement of molecular chains in the case of

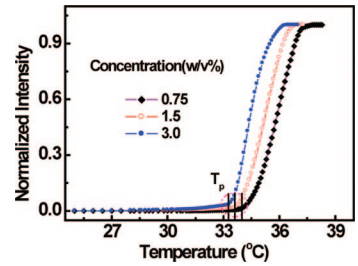

Figure 5. Temperature dependences of normalized RS intensities (at the maximum scattering wavelength) of PVME solutions. The normalized intensity (I_N) is obtained from $I_N = (I - I_{min})/(I_{max} - I_{min})$, where I_{min} and I_{max} are the minimum and maximum values of RS intensities at the maximum scattering wavelength.

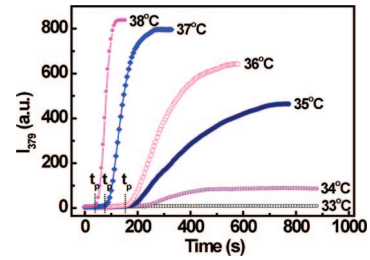

Figure 6. Time dependence of I_{379} of PVME solution (C = 0.75 w/v %) at constant temperatures.

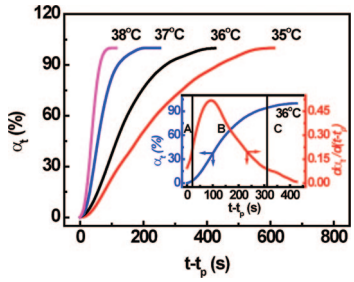

Figure 7. Time dependences of relative extent of phase separation of PVME solution (C = 0.75 w/v %) at different temperatures.

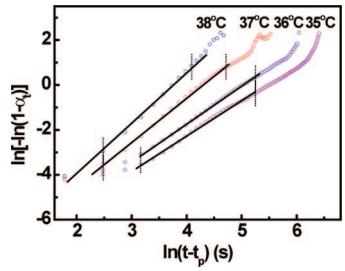

Figure 8. Avrami plots of isothermally phase-separated PVME solution (C = 0.75 w/v %) measured by RS method.

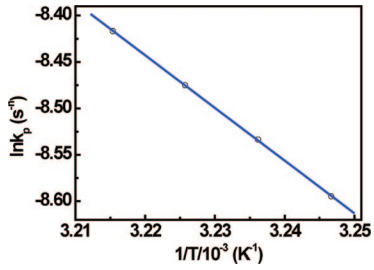

Figure 9. Plot of ln k_p of PVME solution (C = 0.75 w/v %) against the reciprocal of temperature.

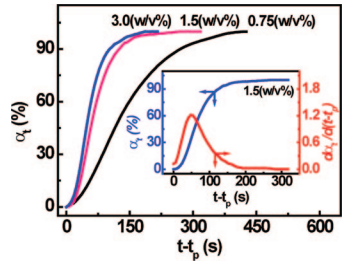

Figure 10. Time dependence of relative extent of phase separation of PVME solutions at 36 °C.

high concentration. As a result of enhanced polymer−polymer interaction, aggregation of PVME chains is favored at lower temperature.

Kinetics of Phase Separation in PVME Solution. In the above sections, the mechanism involved in phase separation of PVME solution has been clarified. On this basis, dynamic process of the phase separation can be inspected by investigating time dependence of the intensity of RS spectrum. It will reveal kinetics information about molecular aggregation in the solution.

To conduct the measurement, the sample cell was put into the single cell Peltier holder at fixed temperature (33, 34, 35, 36, 37, 38 °C, respectively), and kept for 20 s. Afterward, RS spectra of PVME solution (C = 0.75 w/v %) were measured. Figure 6 shows that most time dependences of I_{379} have S-shape profile, except that collected at 33 °C being independent of time

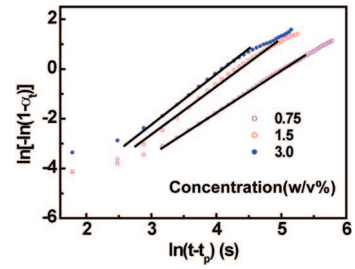

Figure 11. Avrami plots of isothermally phase-separated PVME solutions with different concentrations measured by the RS method.

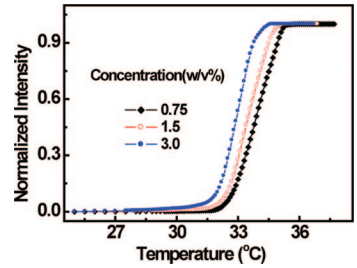

Figure 12. Plots of the normalized intensities of RS (at the maximum scattering wavelength) of PVME solutions against temperature during cooling.

Table 1. Phase Separation Kinetics Parameters of PVME Solution (C = 0.75 w/v %) Determined by the RS Method

T (°C)	t_p (s)	k_p (s^{-n})	n	A (s^{-n})	E_a (kJ/mol)
35	160	1.85×10^{-4}	1.58	1.88×10^4	47.2
36	154	1.97×10^{-4}	1.68		
37	76	2.08×10^{-4}	1.95		
38	40	2.21×10^{-4}	2.23		

Table 2. Phase Separation Kinetics Parameters of PVME Solutions with Different Concentrations at 36°C Determined by RS Method

C (w/v %)	T (°C)	t_p (s)	k_p (s^{-n})	n
0.75		154	1.97×10^{-4}	1.68
1.5	36	82	2.19×10^{-4}	1.93
3.0		52	2.32×10^{-4}	2.02

owing to the absence of phase separation. With a rise in temperature, the curve slope gradually increases due to increase in the rate of phase separation. Similarly, the onset times of phase separation (t_p) estimated from the points on the curves where the RS intensities begin to increase visibly indicate that the phase separation takes less time when temperature is raised. In such a case, the rate of diffusion and aggregation of molecular chains are enhanced at higher temperature, and collision probability of the globules is also increased, so that phase separation is accelerated.

Hereinafter, relative extent of phase separation at constant temperature is calculated[49] to perform a quantitative analysis of the dynamics of this system.

$$\alpha_t = (R_t - R_{t_p})/(R_\infty - R_{t_p}) \quad (3)$$

where α_t is the relative extent of phase separation at time t; R_t and R_{t_p} are RS relative intensities at time t and t_p, respectively; R_∞ is the maximum relative intensity during the phase separation. The relative intensity is calculated from: $R = I_t/I_\infty$, where I_t and I_∞ are RS intensities at the maximum scattering wavelength for PVME solution in which the phase separation is performed at time t and ∞, respectively. I_t/I_∞ of the samples with the same degree of phase separation are identical, regardless of the ways of formation of phase separation.

By means of eq 3 and the experimental data in Figure 6, the time dependences of relative extent of phase separation of

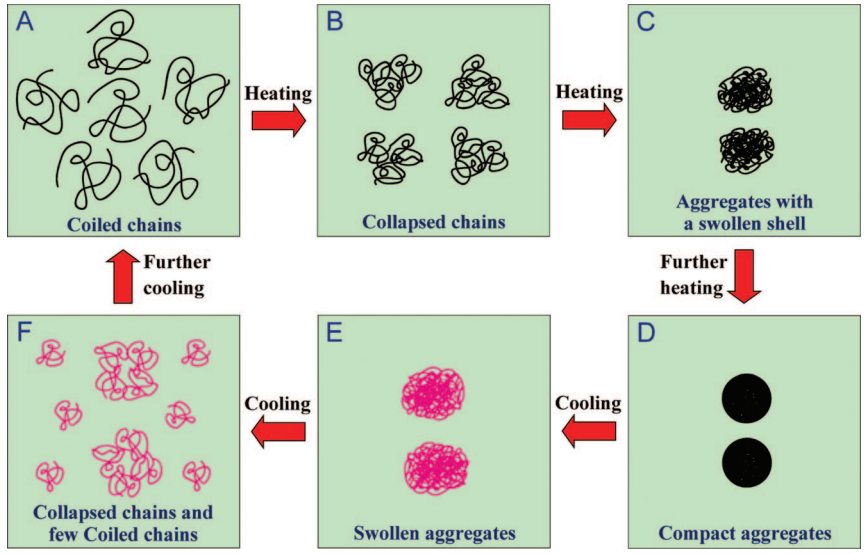

Figure 13. Schematic representation of the phase separation process of poly (vinyl methyl ether) aqueous solution during one heating and cooling cycle.

PVME solution are yielded (Figure 7). From the derivative of α_t with respect to time (see the inset of Figure 7), the three parts of the kinetic process of phase separation can be determined: A, initial stage; B, primary stage; C, late stage.[50]

It is known that the common approach for describing isothermal crystallization kinetics is the Avrami model. When the relative crystallinity is replaced by the relative extent of phase separation at time t, the kinetics of phase separation would be depicted:

$$\ln[-\ln(1-\alpha_t)] = \ln k_p + n \ln(t - t_p) \quad (4)$$

where k_p and n are rate constant and the Avrami exponent, respectively. Both k_p and n can be obtained from the linear regression curve of $\ln[-\ln(1-\alpha_t)] \sim \ln(t-t_p)$.

According to refs 26 and 51, the temperature limits of the metastable region of PVME solution (C = 0.75 w/v %) approximately range from 34 to 39 °C. Besides, as temperature is below 34 °C, the solution lies in the stable region. Clearly, phase separation of the solution under different testing temperatures (35, 36, 37, 38 °C) occurs in the metastable region of the phase diagram, which is the region between binodal and spinodal curves. It means that phase separation of the system occurs by the mechanism of nucleation and growth. Figure 8 shows the Avrami plots of isothermally phase-separated PVME solution (C = 0.75 w/v %) at different temperatures measured by RS method. It can be seen that the plots distinguish primary phase separation from late stage phase separation. That is, phase separation at linear portion represents primary phase separation, while late stage phase separation occurs at nonlinear portion. As only the kinetics of primary phase separation is focused, the best-fit lines are drawn except the initial points in phase separation and the points (deviating from the linearity) of the late stage. Nevertheless, the Avrami plots reveal the distinct three parts, which correspond to the stages of phase separation on the $\alpha_t \sim (t - t_p)$ plot (see the inset of Figure 7). It is evident that the phase separation undergoes induction and accelerating and decelerating growth periods.

Figure 9 presents the plot of ln k_p of the PVME solution (C = 0.75 w/v %) against the reciprocal of temperature. According to Arrhenius equation, apparent activation energy of phase separation is obtained from the slope of the straight line in the chart. Meanwhile, the preexponential factor is calculated from the intercept. Table 1 lists all the kinetic parameters of phase separation of this solution.

Scheme 1. Schematic Representation of the Chemical Structure of PVME Molecule

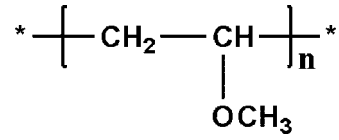

Figure 10 displays time dependences of relative extent of phase separation of PVME solutions with different concentrations at 36 °C. With increasing the concentration, the onset time of phase separation is shortened. This is due to the overlap and entanglement of molecular chains under higher concentration, which facilitates chain aggregation above T_p.

Following the same procedures, Avrami plots of isothermally phase-separated PVME solutions with different concentrations measured by RS method can be drawn (Figure 11). The three parts of phase separation process are also distinctly perceived. Table 2 lists the kinetic parameters of PVME solutions as a function of concentration. It is seen that the rate constant k_p increases with a rise in concentration.

RS of PVME Solutions during Cooling. To have comprehensive knowledge of phase separation of PVME solutions, RS spectra of the solution during cooling were recorded. Again, the plots of normalized intensities of RS (at the maximum scattering wavelength) of PVME solutions against temperature having S-shaped profile are observed (Figure 12). Compared with the curves in Figure 5 that were collected during heating, it is seen that those in Figure 12 shift to lower temperature regime, in the case of identical concentration. This should originate from the formation of intrachain and interchain quasi-hydrogen bonds between different chain segments when they are overlapped in the collapsed state.[52] The quasi-hydrogen bonds can be gradually removed during cooling. As a result of the interchain interaction that is established in the collapsed state at higher temperature, the chain aggregates are swelled, but they do not dissociate at the initial stage of cooling. In addition, the rate at which the polymer chains disengage themselves from the swollen phase-liquid interface would also affect the dissolution rate in polymeric systems.[53−55] Therefore, hysteresis is detected and the curves in Figure 5 and Figure 12 do not overlap.

Conclusions

In this work, RS technique was used to investigate phase separation process of PVME aqueous solutions. The onset temperatures of phase transitions were identified, and the apparent activation energy of phase separation of PVME solution was obtained by kinetics analysis. Moreover, the RS spectra provided information about conformational change and aggregation process of PVME solutions (Figure 13). On the one hand, heating results in coil-to-globule transition and aggregation of PVME chains. When the solution is heated above the microphase transition temperature, PVME chains simultaneously undergo intrachain contraction and interchain association/entanglement, forming large and dense aggregates whose size increases with the solution temperature.[56] The conformation of flexible linear molecular chains changes from expanded coils to collapsed globules during heating, and then the globules become more compact with a rise in temperature. On the other hand, cooling leads to swelling and dissociation of globules. At the initial stage of cooling, the chain aggregates are swelled, but do not begin to dissociate. This reveals that some interchain interaction is formed in the collapsed state at higher temperature.[52] As the solution temperature is further decreased, the aggregates begin to dissociate and the hysteresis gradually disappears. Finally, the conformation of molecular chains returns to its original state at lower temperature.

A new characterization technique for studying phase separation of polymer solutions or blends in terms of RS spectra might thus be developed on the basis of the above findings. Besides, the RS spectra can provide abundant information of the interaction between two different macromolecules, and reveal the internal mechanism of the interaction. Because of its sensitivity, it might be utilized to study kinetics of crystallization of polymers.

Acknowledgment. X.D.C. acknowledges the financial support from the program of National Natural Science Foundation of China (Grant No. 50673104) and Natural Science Foundation of Guangdong Province (Grant No. 7003702).

References and Notes

(1) Katsumoto, Y.; Tanaka, T.; Sato, H.; Ozaki, Y. *J. Phys. Chem. A* **2002**, *106*, 3429–3435.
(2) Fujishige, S.; Kubota, K.; Ando, I. *J. Phys. Chem.* **1989**, *93*, 3311–3313.
(3) Wang, X. H.; Qiu, X. P.; Wu, C. *Macromolecules* **1998**, *31*, 2972–2976.
(4) Lee, L. T.; Cabane, B. *Macromolecules* **1997**, *30*, 6559–6566.
(5) Kjellander, R.; Florin, E. *J. Chem. Soc., Faraday Trans.* **1981**, *77*, 2053–2077.
(6) Ataman, M. *Colloid Polym. Sci.* **1987**, *265*, 19–25.
(7) Karlstroem, G. *J. Phys. Chem.* **1985**, *89*, 4962–4964.
(8) Maeda, Y. *Langmuir* **2001**, *17*, 1737–1742.
(9) Horne, R. A.; Almeida, J. P.; Day, A. F.; Yu, N. T. *J. Colloid Interface Sci.* **1971**, *35*, 77–84.
(10) Schafer-Soenen, H.; Moerkerke, R.; Berghmans, H.; Koningsveld, R. *Macromolecules* **1997**, *30*, 410–416.
(11) Vakkalanka, S. K.; Brazel, C. S.; Peppas, N. A. *J. Biomater. Sci., Polym. Ed.* **1996**, *8*, 119–129.
(12) Gupta, P.; Vermani, K.; Garg, S. *Drug Discovery Today* **2002**, *7*, 569–579.
(13) Spěváček, J.; Hanyková, L.; Starovoytova, L. *Macromolecules* **2004**, *37*, 7710–7718.
(14) Yang, Y. Y.; Zeng, F.; Xie, X. L.; Tong, Z.; Liu, X. X. *Polym. J.* **2001**, *33*, 399–403.
(15) Maeda, H. *J. Polym. Sci., Part B: Polym. Phys.* **1994**, *32*, 91–97.
(16) Zeng, X. G.; Yang, X. Z. *J. Phys. Chem. B* **2004**, *108*, 17384–17392.
(17) Gu, W. X.; Wu, P. Y. *Anal. Sci.* **2007**, *23*, 823–827.
(18) Swier, S.; Van Durme, K.; Van Mele, B. *J. Polym. Sci., Part B: Polym. Phys.* **2003**, *41*, 1824–1836.
(19) Moerkerke, R.; Koningsveld, R.; Berghmans, H.; Dušek, K.; Šolc, K. *Macromolecules* **1995**, *28*, 1103–1107.
(20) Moerkerke, R.; Meeussen, F.; Berghmans, H.; Koningsveld, R.; Mondelaers, W.; Schacht, E.; Dušek, K.; Šolc, K. *Macromolecules* **1998**, *31*, 2223–2229.
(21) Van Durme, K.; Loozen, E.; Nies, E.; Van Mele, B. *Macromolecules* **2005**, *38*, 10234–10243.
(22) Maeda, Y.; Mochiduki, H.; Yamamoto, H.; Nishimura, Y.; Ikeda, I. *Langmuir* **2003**, *19*, 10357–10360.
(23) Maeda, Y.; Yamamoto, H.; Nishimura, Y.; Ikeda, I. *Langmuir* **2004**, *20*, 7339–7341.
(24) Spevacek, J.; Hanykova, L. *Macromolecules* **2005**, *38*, 9187–9191.
(25) Jinnai, H.; Smalley, M. V.; Hashimoto, T.; Koizumi, S. *Langmuir* **1996**, *12*, 1199–1203.
(26) Nies, E.; Ramzi, A.; Berghmans, H.; Li, T.; Heenan, R. K.; King, S. M. *Macromolecules* **2005**, *38*, 915–924.
(27) Nies, E.; Li, T.; Berghmans, H.; Heenan, R. K.; King, S. M. *J. Phys. Chem. B* **2006**, *110*, 5321–5329.
(28) Luo, H. Q.; Liu, S. P.; Liu, Z. F.; Liu, Q.; Li, N. B. *Anal. Chim. Acta* **2001**, *449*, 261–270.
(29) Liu, S. P.; Chen, Y. H.; Liu, Z. F.; Hu, X. L.; Wang, F. *Microchim. Acta* **2006**, *154*, 87–93.
(30) Chen, Y. H.; Gao, D. J.; Tian, Y.; Ai, P.; Zhang, H. Q.; Yu, A. M. *Spectrochim. Acta A* **2007**, *67*, 1126–1130.
(31) Qi, L.; Han, Z. Q.; Chen, Y. *J. Chromatogr. A* **2006**, *1110*, 235–239.
(32) Jiang, Z. L.; Liu, S. P.; Zhao, B. G.; Chen, S.; Li, J. A. *Spectrosc. Spect. Anal.* **2002**, *22*, 615–618.
(33) Pasternack, R. F.; Schaefer, K. F.; Hambright, P. *Inorg. Chem.* **1994**, *33*, 2062–2065.
(34) Huang, C. Z.; Li, K. A.; Tong, S. Y. *Bull. Chem. Soc. Jpn.* **1997**, *70*, 1843–1849.
(35) Huang, C. Z.; Pang, X. B.; Li, Y. F.; Long, Y. J. *Talanta* **2006**, *69*, 180–186.
(36) Lu, W.; Fernández Band, B. S.; Yu, Y.; Li, Q. G.; Shang, J. C. *Microchim Acta* **2007**, *158*, 29–58.
(37) Pasternack, R. F.; Bustmante, C.; Collings, P. J.; Giannetto, A.; Gibbs, E. J. *J. Am. Chem. Soc.* **1993**, *115*, 5393–5399.
(38) Pasternack, R. F.; Collings, P. J. *Science* **1995**, *269*, 935–939.
(39) Zhang, Y. H. *Physical Chemistry*; Shanghai Jiao Tong University Press: Shanghai, 1988.
(40) Sonnenschein, M. F.; Roland, C. M. *J. Polym. Sci., Part B: Polym. Phys.* **1991**, *29*, 431–436.
(41) Guo, Y. L.; Sun, B. J.; Wu, P. Y. *Langmuir* **2008**, *24*, 5521–5526.
(42) De Paula, J. C.; Robblee, J. H.; Pasternack, R. F. *Biophys. J.* **1995**, *68*, 335–341.
(43) Tanaka, H. *Phys. Rev. Lett.* **1994**, *72*, 1702–1705.
(44) Tanaka, H. *J. Chem. Phys.* **1996**, *105*, 10099–10114.
(45) Tanaka, H. *J. Chem. Phys.* **1997**, *107*, 3734–3737.
(46) Fialkowski, M.; Holyst, R. *Macromol. Theory Simul.* **2008**, *17*, 263–273.
(47) Hanyková, L.; Spěváček, J.; Ilavský, M. *Polymer* **2001**, *42*, 8607–8612.
(48) Spěváček, J.; Hanyková, L.; Ilavský, M. *Macromol. Symp.* **2001**, *166*, 231–236.
(49) Lee, K. D.; Chan, P. K.; Feng, X. S. *Macromol. Theory Simul.* **2003**, *12*, 413–424.
(50) Lee, K. D.; Chan, P. K.; Feng, X. S. *Macromol. Theory Simul.* **2002**, *11*, 996–1005.
(51) Bergé, B.; Koningsveld, R.; Berghmans, H. *Macromolecules* **2004**, *37*, 8082–8090.
(52) Cheng, H.; Shen, L.; Wu, C. *Macromolecules* **2006**, *39*, 2325–2329.
(53) Brochard, F.; de Gennes, P. G. *Physicochem. Hydrodyn.* **1983**, *4*, 313–322.
(54) Devotta, I.; Ambeskar, V. D.; Mandhare, A. B.; Mashelkar, R. A. *Chem. Eng. Sci.* **1994**, *49*, 645–654.
(55) Devotta, I.; Premnath, V.; Badiger, M. V.; Rajmohanan, P. R.; Ganapathy, S.; Mashelkar, R. A. *Macromolecules* **1994**, *27*, 532–539.
(56) Ye, J.; Xu, J.; Hu, J. M.; Wang, X. F.; Zhang, G. Z.; Liu, S. Y.; Wu, C. *Macromolecules* **2008**, *41*, 4416–4422.

MA802671A